Construction and Building Materials 173 (2018) 452–460

Contents lists available at ScienceDirect

Construction and Building Materials

journal homepage: www.elsevier.com/locate/conbuildmat

Sacrificial mortars for surface desalination

N. Husillos-Rodríguez [a], Paula María Carmona-Quiroga [a], S. Martínez-Ramírez [b,*], M.T. Blanco-Varela [a], R. Fort [c]

[a] Instituto de Ciencias de la Construcción Eduardo Torroja (IETCC-CSIC), C/Serrano Galvache 4, 28033 Madrid, Spain
[b] Instituto de Estructura de la Materia (IEM-CSIC), C/Serrano 121, 28006 Madrid, Spain
[c] Instituto de Geociencias (IGEO-CSIC, UCM), C/Doctor Severo Ochoa 7, 28040 Madrid, Spain

HIGHLIGHTS

- Four absorbent mortars were designed and used as sacrificial desalinating media.
- The salts elimination was most effective in anions with a smaller ionic volume.
- Effectiveness increases with high superficial salt concentration.
- Three years later, the salt concentration was 50% lower than prior to treatment.

GRAPHICAL ABSTRACT

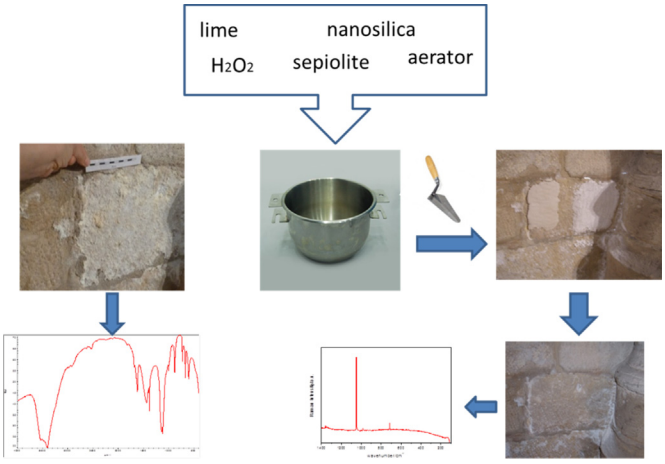

ARTICLE INFO

Article history:
Received 19 April 2017
Received in revised form 22 December 2017
Accepted 3 April 2018
Available online 24 April 2018

Keywords:
Desalination
Lime mortars
Sepiolite
Nanosilica
Dolostone
Heritage conservation

ABSTRACT

Four absorbent mortars were designed in this study and used as sacrificial desalinating media. The mortars comprised lime, sepiolite, nanosilica (72/3/25 by weight) and three admixtures (H_2O_2 and two commercial aerators) and had a liquid/solid ratio of 0.9, a mean porosity of 40% and a mean pore size of 0.8–0.7 μm. These mortars were applied three times to ashlars exhibiting surface saline efflorescence on a church at Talamanca del Jarama, a town in the Spanish province of Madrid. The salts impregnating the wall were characterised with XRD, FTIR and Micro-Raman spectroscopy. The ion concentrations in the ashlars was studied with ion chromatography at 0.5 cm, 1.5 cm and 3.0 cm from the surface after each application and the inner and outer surfaces of the mortars were analysed with Micro-Raman spectroscopy to determine the desalinating efficacy of the mortars.

The mortars designed mobilised and absorbed the soluble salts in the ashlars; as a rule, elimination was most effective in anions with a smaller ionic volume and therefore greater ionic mobility and when the salt concentration was high and superficially located. Three years after application of the desalinating mortars, the salt concentration in the ashlars treated was 50% lower than prior to treatment.

* Corresponding author.
E-mail address: sagrario.martinez@csic.es (S. Martínez-Ramírez).

https://doi.org/10.1016/j.conbuildmat.2018.04.029
0950-0618/

1. Introduction

One of the most prominent causes of built heritage decay is the presence of salts in the materials [1,2]. Such salts may crystallise on the surface of (saline efflorescence) or inside (sub- and crypto-efflorescence) materials, to the detriment of the value of the heritage asset. The effect of the former is essentially aesthetic, whereas the latter affects dimensional stability. When the crystallisation pressure exerted by a salt exceeds the mechanical strength of a material, the latter cracks, scales, flakes or crumbles.

Salts also hamper asset restoration and conservation, for they limit the effectiveness of consolidation and water-repellency treatments [3]. Hence the importance of establishing their presence in buildings, determining their origin, assessing their implications for decay and defining the most suitable elimination technique. Such techniques depend on the location of the salts in the walls, their chemical and mineralogical composition and the microclimate prevailing in the area surrounding the materials affected [4]. The petrophysical properties of the material housing salts must also be established, for factors such as porosity and pore size distribution affect salt concentration [5–8]. Some salts undergo mineralogical transformation when the relative humidity (RH) and temperature (T) of the surrounds vary. That, in turn, often induces volume change and the concomitant damage to the material [9–12]. Prior to any intervention, the superficial salts must be eliminated from the areas involved and their presence inside the walls must be lowered with the techniques presently available [13].

The origin of salts varies depending on their location and determines the most suitable desalinating technique. If the salts are found in depth, the origin may be attributed to human activity, certain types of mortars, underground water or the material itself. The desalination methods most commonly used in such cases are poultices, sacrificial mortars and immersion or electrochemical techniques.

If the salts are located near or on the surface, their source may be, in addition to the above, air pollution or microorganisms; in such cases they are eliminated primarily with mechanical, chemical or laser methods.

Despite the variety of methods in place to extract soluble salts [14–17], they are often scantly effective or inviable. None serves for all manner of materials, the results are questionable [18] and none is able to wholly eliminate salts deep within walls [19]. Very few studies have been conducted on the effectiveness of salt reduction in situ due primarily to the difficulty of assessing the findings, for the samples that would be needed cannot always be collected for analysis in light of the heritage value of the element to be conserved. To assess salt extraction efficiency, the pre- and post-treatment salt concentration must be determined. Efficacy is not the same on the substrate surface as at greater depths [19].

The environmental conditions (RH, T) that prevent salt mobility must also be established and the source of the salt eliminated, for otherwise it will re-impregnate the area to be protected [20].

One of the techniques for removing salt from inside walls is the application of sacrificial mortars [21–23]. Lime mortar porosity can be modified by adding appropriately structured inert or pozzolanic materials or admixtures. Sepiolite is known to be highly absorbent and to raise lime mortar porosity when added at concentrations of over 1% [24]. Lime mortars with 5% sepiolite have been shown to be more absorbent than the same mortars without the addition [25]. Other types of additions as amorphous silica added to lime mortars produce C-S-H gel by pozzolanic reaction, which modify the mortar microstructure as well as adherence and mechanical properties [26,27]. Finally, admixtures such as aerators are often used to increase the porosity of mortars and concretes [28]. From Keertana [29] a gas produced by hydrogen peroxide in the mortar improves the homogeneity of the void structure.

Based on the knowledge of the changes in lime mortar absorptivity and microstructure induced by sepiolite and nanosilica, this study was aimed at designing a sacrificial mortar able to absorb salts present in stone. Such mortars must be highly absorbent and exhibit low strength and suitable bondability while actively extracting salts, but must be readily removable with the least possible damage to the substrate after fulfilling their purpose.

The mortars designed were applied to dolostone ashlars located in the internal wall of the apse of a church at Talamanca del Jarama, a town in the Spanish province of Madrid. That stone, that is scantly resistant to salt crystallisation, has 15–150 μm crystals, a porosity of 16.2 ± 3.4, an average pore size of 0.43 μm and a pore size distribution ranging primarily from 0.1 μm to 10 μm being its water absorption coefficient of 86 $g \cdot m^{-2} \cdot s^{-0.5}$ [30,31].

The mentioned ashlars were covered by saline efflorescences which not only result in aesthetical effects but also in surface cohesion less.

2. Experimental procedure

2.1. Materials, mortar optimisation

Tests were conducted on mortars containing different proportions of lime, sepiolite (with two particle size distributions, 15/30 and 6/30), nanosilica, and three modifiers of porosity, two commercial admixtures (SR and SG 500), and H_2O_2.

2.1.1. Raw materials

a) Hydrated lime (CL90-S).
b) Two types of commercial sepiolite with the following information supply from the manufacturer: **15/30** with 95% ranging from 1.7 mm to 0.25 mm and 130% water absorption and **6/30** (70% pure), 14.7 wt% < 600 μm; 70 wt% from 600 μm to 4.7 mm; 5.5 wt% > 4.75 mm; 95% water absorption and BET SS 240 m^2/g.
c) Amorphous nanosilica consisting primarily of amorphous SiO_2 (~90%) with a loss on ignition at 1000 °C of 8.9% (free water and OH from silanol groups) [26].
d) Aerators: a) SR (lignosulphonate base) and SG 500 (triisopropilamine base), both aerators used to add air to mortars, calling for 0.20–0.40 g per 225 g of mixing water to have a perceptible effect. B) H_2O_2 (Panreac commercial hydrogen peroxide) with a molecular weight of 34.01 g; 0.5% non-volatile matter; 0.001% sulfates; 0.00005% As; 0.001% Ni; 0.001% Cu; 0.001% Pb; and 0.005% Fe. Aerators were incorporated in the mixing water.

2.1.2. Optimisation of sacrificial mortars

Lime and sepiolite compositions were homogenised in the mixer-bowl before the incorporation of the water with aerators in solution. The mortars were obtained initially by mixing lime, the two types of sepiolite and H_2O_2 (to improve the homogeneity of the void structure) in different proportions (M1, M2, M5, M6 in Table 1). The mortars were elaborated by moulding a series of six 6 × 7 × 1 cm prismatic specimens per composition, cured for 3 days at 21 ± 1 °C and RH > 95%.

All the specimens shrank and cracked even under the high humidity conditions described, with greater shrinking at higher doses of H_2O_2. With a view to attaining dimensional stability and raising mechanical strength, nanosilica was added to the mortars and the moulds were sealed with a film during initial curing (M3, M4, M7, M8 in Table 1). After 3 days the moulds were taken from the chamber and after removing the film they were stored at laboratory temperature and a RH of 50–65% for 7 days. When

Table 1
Batching for desalinating mortars with different types of sepiolite, with or without admixtures, nanosilica and H_2O_2 (g).

Mortar	Lime (g)	Sep (g) **(15/30)**	Sep (g) **(6/30)**	H_2O_2 (g)	nSA (g)	H_2O (g)
M1	75		25			90
M2	75		25	0.5		89.5
M3	72		25		3	90
M4	72		25	0.5	3	89.5
M5	75	25				90
M6	75	25		0.2		89.8
M7	72	25			3	90
M8	72	25		0.2	3	89.8

Table 2
Batching for desalinating mortars with sepiolite 15/30 and nanosilica, with or without admixtures and H_2O_2 (g).

Mortar	Lime (g)	Sep (g) (15/30)	H_2O_2 (g)	SR (g)	SG-500 (g)	nSA (g)	H_2O (g)
M13	72	25	1			3	89
M14	72	25	0.5			3	89.5
M15	72	25	0.5	0.2		3	89.3
M16	72	25		0.2		3	89.8
M17	72	25		0.2	0.16	3	89.64

they were subsequently removed from the moulds no dimensional change was observed. While the specimens with the coarser sepiolite (6/30) did not crack, they broke when removed from the moulds and the ones containing hydrogen peroxide were very weak, so that sepiolite (6/30) was discarded.

Of the specimens made with sepiolite 15/30 only number 7, which contained nanosilica but no H_2O_2, exhibited suitable consistency. In order to try to raise mortar porosity two aerators SR and SG-500 were added while the L/S ratio was 0.9 throughout.

As all the mixes listed in Table 2 contained nanosilica and H_2O_2 and/or an admixture and could be suitably removed from the moulds, they were chosen, together with specimen 7 (in Table 1), to continue the study. Admixtures SR and SG-500 were added to raise mortar porosity and the L/S ratio was 0.9 throughout.

Mortars M7, M13, M14, M15, M16 and M17 were sealed with a film, cured for 24 h in a humidity chamber and subsequently air dried under laboratory conditions (≈24 °C, RH = 60%). All the mortars lost 45–50% of their weight in the first 96 h, after which the values stabilized, thus indicating the minimum time they would need to be kept in situ.

A bonding test was also conducted, vertically applying approximately 2 cm thick layers of mortar to a moist brick. Only the mortars sealed with a film for 24 h remained attached to the substrate until the end of the test time (7 days), although after 4 days they began to become detached around the edges. All the mortars could be removed by hand with no need for any tool whatsoever.

The mortars sealed with film, cured for 24 h in a humidity chamber and subsequently air-dried for 7 days in the laboratory were tested for low pressure water absorption. The mortars with admixtures (M15, M16 and M17) were likewise tested with water and a 4 wt% Na_2SO_4 solution for absorptivity. Sodium sulfate was chosen since is one of the salts found in the efflorescences, and the mobility of its anion is low due to its large size.

2.2. Application of mortars to a salt-containing wall

The mortars designed were applied three times to dolostone ashlars located in the internal wall of the apse a church at Talamanca del Jarama, a town in the Spanish province of Madrid. The selected interior south wall suffer an important thermal variation due to the intense insolation of its external face favouring wet/dry cycles and salts crystallisation processes[32]. The temperature outside the church in days of June reaches values of 41.6 °C, while in the interior the average value is of 27.4 °C, which gives a thermal variation of −14.2 °C. In December the thermal variation is only 0.2 °C (indoor temperature 11.3 °C and outdoor temperature of 11.3 °C). This variation is different at different heights of the wall in which the sacrificial mortars were applied, being for the summer months and at 40 cm of height it was −17.2 °C. It is in these levels where the highest humidity is also detected inside the walls due to the absorption of capillary water [32].

The mortars were applied on ashlars at 40 cm over soil, after mechanical cleaning of surface saline efflorescences. The selected areas were cleaned with a scouring brush and the efflorescences collected. Four of the sacrificial mortars designed were laid on the brushed stone to a thickness of approximately 2 cm and left for 10 days, after which they were removed.

The mortars were applied a further three times and the surface composition of the inner (in contact with the wall) and outer faces of the mortars, after the first and the third application was studied by Micro-Raman spectroscopy to determine their desalinating capacity.

Fig. 1 shows the stone before and after brushing and prior to applying the mortar.

2.3. Analytical methodology

The raw materials were characterised mineralogically and physically.

The lime and sepiolite were analysed on a Bruker D8 Advance X-ray diffractometer fitted with a high voltage, 2.2 kW generator and a (CuKα1 1.5406 Å and CuKα2 1.5444 Å) copper anode X-ray tube normally operating at 40 kV and 30 mA. The scanning range was $2\theta = 5°–60°$ with a (2θ) step size of 0.02°.

Lime thermal behaviour was studied with differential thermal and thermogravimetric analysis (DTA/TG), heating specimens at a rate of 10 °C/min to a maximum temperature of 1050 °C in N_2 and air atmospheres on a TA Instruments SATQ600 analyser.

Lime and sepiolite specific surface were obtained by Brunauer-Emmett-Teller (BET)-specific surface method, from nitrogen adsorption isotherms generated by a Micromeritics ASAP 2010 analyser.

The lime particle size distribution was found with laser diffraction on a Sympatec Helos 12LA particle analyser fitted with wet and dry dispersion systems and featuring a measuring range of 0.1–175 μm.

Low water pressure absorption values were found for the mortar specimens as recommended in European standard EN

Fig. 1. Stone prior to application of the mortars: a) and c) before, and b) and d) after removing efflorescences.

16302:2012 [33]. Determination of water absorption coefficient by capillarity was carried out by UNE-EN 1925:1999 [34]; in addition this coefficient was also determined using a 4% Na_2SO_4 solution in order to estimate if the mortars were able to absorb anions with reduced mobility (minor than the chloride one for example) due to its large ionic volume. Coefficient of saturation of water was determined by Rilem recommendation [35]. Mercury Porosity was determined with a Micromeritics Autopore IV 9500.

The raw materials, efflorescences and desalinating mortars before and after the first and the third applications were scanned on a Renishaw Raman InVia spectrometer fitted with an electrically cooled CCD camera. The excitation source was a frequency-doubled Nd:YAG laser, supplying a 25 mW beam at a wavelength of 785 nm. The spectral resolution was set in all cases to 2 cm^{-1}. Raman spectra, which consisted of a single span, were recorded with a total acquisition of 10 s.

The salt content inside the wall after cleaning the surface and removing the mortars after each application was determined by taking samples at depths of 0.5 cm, 1.5 cm and 3 cm with an 8 mm bit. The samples (0.1 g approximately) were dissolved in 10 mL of Milli-Q ultrapure water and immersed for 45 min in an ultrasonic bath (Selecta model Ultrasounds-H) at 60 °C and centrifuged in a Heareaus Thermo model Labofuge 400 device for 2 min at 3500 rpm and a relative centrifugal force (rcf) of 3400. After the mortars were removed, their soluble salt anion content was quantified on a Metrohm 761 Compact IC ion chromatograph.

3. Results and discussion

3.1. Characterisation of raw materials

The following crystalline phases were identified on the XRD pattern for the lime sample studied: portlandite [$Ca(OH)_2$] (most intense reflections), calcite [$CaCO_3$], much smaller proportions of CaO and traces of anhydrite. The DTA/TG analysis of the lime (Table 3) yielded three endothermal signals: at 48 °C, attributed to the loss of moisture; at 674 °C, to the thermal decomposition of $CaCO_3$; and at 449 °C (the most intense signal), to portlandite dehydroxylation. By the end of the test the total mass loss amounted to 24.5%. The lime contained 84.8% $Ca(OH)_2$ and 5.8% $CaCO_3$.

Further to the particle size distribution curve, the mean particle size was 4.4 μm, with 90% of the particles smaller than 13.5 μm (Fig. 2 and Table 4).

The XRD patterns of the studied sepiolite samples included, in addition to the pertinent reflections (2θ = 9.4°), also traces of quarzt (SiO_2).

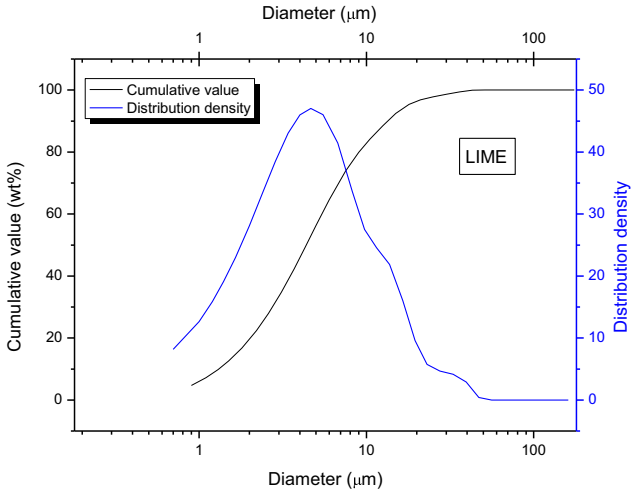

Fig. 2. Particle size distribution curve for lime.

Table 4
Lime particle diameters below which 10%, 50% and 90% of the sample mass was observed to lie.

Sample D (μm)	10% of the particles	50% of the particles	90% of the particles
Lime	<1.31	<4.38	<13.48

The BET specific surface of the amorphous silica was a very high 371 ± 2 m^2/g, while its particle size was under 30 nm as determined by transmission electron microscopy (TEM) [26].

3.2. Mortar hydric properties

Fig. 3 shows the low pressure water absorption findings for mortars M7, M13, M14, M15, M16 and M17. M7 was considered as a reference since no aerators were added.

Water absorptivity was high in the first 1000 s in all the materials. Mortars M16 and M17 (neither bearing H_2O_2) absorbed 80% of the water in less than 30 s and completed the test in 300 s. Water was absorbed more quickly in mortars containing H_2O_2 than in the mortar with no admixtures and more slowly than in the mortar with admixture SR only.

Table 3
DTA/TG and quantitative mineralogical data for lime in an air atmosphere.

T (°C)	TG (%)	Enthalpy (J/g)	Loss	Mineralogy (wt%)	
25–300	1.3	92.3	Water		
334–502	20.64	1213	OH^-	$Ca(OH)_2$	84.8
502–1000	2.55	301.4	CO_2	$CaCO_3$	5.8

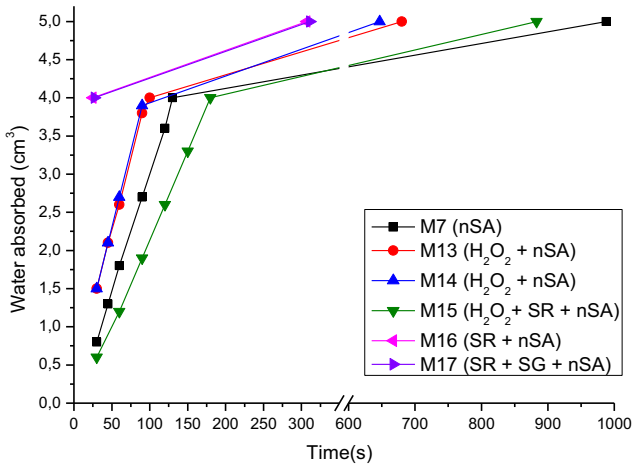

Fig. 3. Water absorbed by the [15/30 lime/nanosilica/sepiolite] mortars surfaces, with and without H_2O_2 and admixtures (SR, SG) vs time.

Table 5
Water saturation coefficients for mortars M15, M16 and M17.

Mortar	M15	M16	M17
Sat. cfnt (%wt)	72.8	90	69.7

The water saturation coefficients for mortars M15, M16 and M17 (with admixtures) (Table 5) ranged from 70% to 90%, with the highest value observed for the mortar containing SR (mortar M16). Adding H_2O_2 or SG 500 lowered the saturation coefficient by approximately 20 points (mortars M15 and M17) (Table 5).

The water absorption coefficients by capillarity of mortars M15, M16 and M17 are listed in Table 6. Results point out that M16 (having only SR admixture) has both the highest water saturation and capillarity coefficients. All mortars saturated practically in the first 5 min of testing, and capillary absorption of a 4 wt% Na_2SO_4 solution was lower than that of water, because of large ionic volume of SO_4^{2-} anions has reduced mobility, except for M15 mortar, which present the lowest porosity and the highest amount of porous >1 μm.

The total porosity of the mortars varied from 41% to 44% (Table 7), whilst the pore size distribution was very similar in mortars M16 and M17, which were more microporous than mortar M15. The mean pore size was: M15 = 0.86 μm, M16 0.74 μm, M17 = 0.72 μm.

On the grounds of their volume stability (they can be demolded without neither cracks or breaks), bondability to the substrate substrate (strong enough to remain joint to substrate for 7 days), facility to be removed (only by hand and almost does not remain any amount of material on substrate after mortar elimination) and high porosity, mortars M14, M15, M16 and M17 were chosen as the best suited for desalination assessment on the walls of the Talamanca del Jarama church.

The composition of the four mortars used is given in Table 8.

3.3. In situ effectiveness of mortars

The XRD, FTIR and Raman analyses showed the efflorescences to consist in sodium and magnesium sulfate in the form of mirabilite ($Na_2SO_4{\cdot}10H_2O$), epsomite ($MgSO_4{\cdot}10H_2O$) and smaller proportions of gypsum ($CaSO_4{\cdot}2H_2O$) and rozenite ($FeSO_4{\cdot}4H_2O$). Nitrates such as nitratite ($NaNO_3$), nitre (KNO_3) and nitromagnesite ($Mg(NO_3)_2{\cdot}6H_2O$) were also identified. Prior studies [36] of the outer side of the apse of the same church identified high gypsum ($CaSO_4{\cdot}2H_20$) and halite (NaCl) concentrations.

Table 6
Capillary water and 4 wt% Na_2SO_4 solution absorption coefficient of mortars M15, M16 and M17.

Mortar	Capillarity coefficient ($g/m^2s^{0.5}$)		
	M15	M16	M17
H_2O	2693.4	3435.1	2831.3
Na_2SO_4	2905.3	2819.2	1239.8

According to the IC anion analysis of the efflorescences, the proportion of chlorides was over two orders of magnitude lower than the other ions and the sulfate concentration in the efflorescences practically doubled the nitrate content ($[SO_4^{2-}]$ = 266 ± 81 ppm; $[NO_3^-]$ = 143 ± 68 ppm and $[Cl^-]$ = 0.96 ± 0.86 ppm).

Figs. 4 and 5 shows the Raman spectra for the inner and outer faces of mortar M15 after the first and third applications, respectively. The information of the application is included in Table 9.

After the first application, salts characteristic of calcite and portlandite appeared on both sides of the mortars, along with signals on the spectra at 990 cm^{-1} and 1050 cm^{-1}. The former was attributed to the presence of a sulfate in the form of epsomite ($MgSO_4{\cdot}7H_2O$) while the latter could be due to an alkaline or alkaline-earth nitrate or a dehydrated magnesium sulfate. Wang et al. [37] reported shifts in the sulfate group ν_1 signal from values near 980 cm^{-1} in decahydrates to 1052 cm^{-1} in anhydrous samples. Nitrates, in turn, have a narrow band in the 1035–1055 cm^{-1} range, the position of which depends on the cation and state of hydration. As $NaNO_3$ exhibits a band at 1067 cm^{-1}, KNO_3 at 1049 cm^{-1}, $Ca(NO_3)_2{\cdot}4H_2O$ at 1051 cm^{-1} and $Mg(NO_3)_2{\cdot}6H_2O$ at 1059 cm^{-1} [37], the band observed was probably generated by a calcium or potassium nitrate. Whilst the FTIR spectrum confirmed the presence of epsomite, the type of nitrates could not be identified with this technique, for the only visible band was the ν_3 asymmetric stretching band for N-O common to all nitrates and located at 1385 cm^{-1}.

The Raman spectra for the outer side of the mortar included bands attributable to gypsum, brucite and perhaps an iron oxide. The absence of such signals on the inner side may denote an ionic exchange between Mg and Ca, as per the following reaction:

$$Ca(OH)_2 + MgSO_4 \cdot 7H_2O \rightarrow Mg(OH)_2 + CaSO_4 \cdot 2H_2O + 5H_2O$$

The magnesium sulfate drawn from the wall reacted with the calcium hydroxide, yielding brucite and gypsum, salts with a much lower solubility than the former salts (solubility at 20 °C: portlandite, 1.48 g/L; $MgSO_4{\cdot}7H_2O$, 362 g/L; brucite, $7.64{\cdot}10^{-3}$ g/L; gypsum, 2.23 g/L).

The presence of calcium nitrate on both sides of the mortars confirmed their ability to extract the nitrate anion, although Na or K cations might have been exchanged for Ca when the (sodium or potassium) nitrates came into contact with the portlandite in the mortar. The wall might, then, have contained Na or K, rather than only Ca nitrates (solubility: $NaNO_3$, 92 g/L; KNO_3, 1800 g/L; $Ca(NO_3)_2$, 1000 g/L).

After the third application, a number of nitrates were observed ($NaNO_3$ and $Ca(NO_3)_2$), along with sulfates (gypsum and magnesium sulfate) on both the inner and outer sides of the mortars, an indication that they continued to remove salts from the ashlar.

The signal at 980 cm^{-1}, already visible, after the first and third applications was became wider after the third one and its peak may have shifted to somewhat higher wavenumbers, possibly denoting a different degree of magnesium sulfate hydration.

Table 9 lists the salts found on the inner and outer sides of the desalinating mortars after each application. Mortars M15 and M14, which contained H_2O_2, eliminated the largest amounts of salt, particularly after the first application.

Table 7
Mercury intrusion porosity data for mortars M14, M15, M16 and M17.

Pore size (μm)	M14		M15		M16		M17	
	Pore volume ($ml/g*10^{-4}$)	Pore Vol. (%)	Pore volume ($ml/g*10^{-4}$)	Pore volume (%)	Pore Volume ($ml/g*10^{-4}$)	Pore volume (%)	Pore Volume ($ml/g*10^{-4}$)	Pore volume (%)
> 100	211	4.5	252	5.5	54	0.5	48	0.4
100–10	573	4.9	589	5.2	296	2.7	245	2.3
10–1	980	8.4	1008	8.9	1038	9.6	880	8.2
1–0.15	2647	22.7	2741	24.3	3354	31.0	3358	31.3
Total	4411	39.5	4590	40.8	4742	43.8	4531	42.3

Table 8
Mortar composition.

Mortar	Composition	M14	M15	M16	M17
Solid (200 g)	Lime (72%)	144 g			
	Nanosilica (3%)	6 g			
	Sepiolite (25%)	50 g			
water + admixtures (180 g)	H_2O	179 g	178.6 g	179.6 g	179.28 g
	H_2O_2 (0.55%)	1 g	1 g	x	x
	SR	x	0.4 g	0.4 g	0.4 g
	SG500	x	x	x	0.32 g

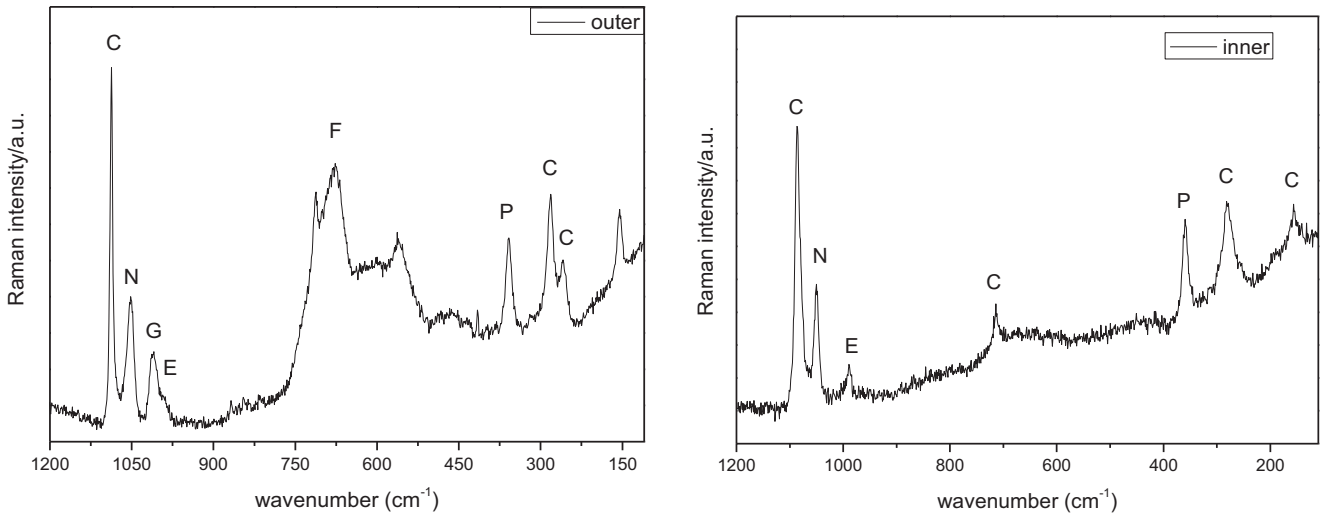

Fig. 4. Micro-Raman spectrum for mortar M15 after the first application; left: outer side of mortar; right: inner side (laser λ = 785 nm). C = Calcite; N = Nitrate; P = Portlandite; E = Epsomite; G = Gypsum; F = Feldspar.

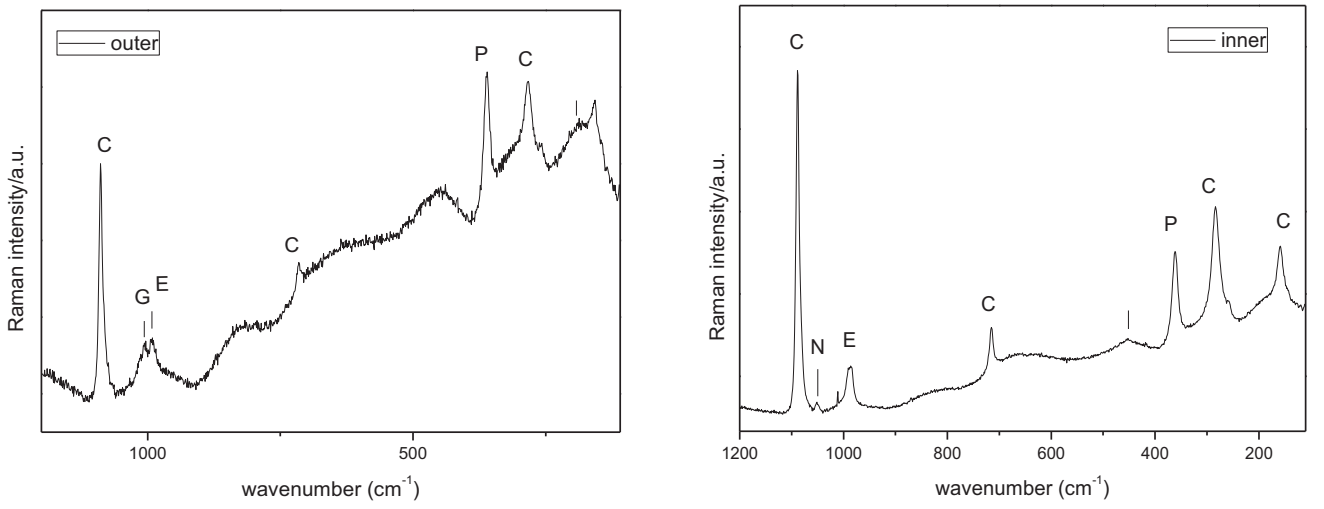

Fig. 5. Micro-Raman spectrum for mortar M15 after the third application; left: outer side of mortar; right: inner side (laser λ = 785 nm). C = Calcite; N = Nitrate; P = Portlandite; E = Epsomite; G = Gypsum.

Table 9
Salts identified by Raman spectroscopy on the inner and outer sides of the mortars after each application.

	1st application		2nd application		3rd application	
	Inner	Outer	Inner	Outer	Inner	outer
M14	$NaNO_3$; $Ca(NO_3)_2{\cdot}4H_2O$ $CaSO_4{\cdot}2H_2O$ $Na_2SO_4{\cdot}10H_2O$	$NaNO_3$; $Ca(NO_3)_2{\cdot}4H_2O$ $CaSO_4{\cdot}2H_2O$ $Na_2SO_4{\cdot}10H_2O$	$NaNO_3$; $Ca(NO_3)_2{\cdot}4H_2O$ $Na_2SO_4{\cdot}10H_2O$	$Na_2SO_4{\cdot}10H_2O$	$Na_2SO_4{\cdot}10H_2O$	$Na_2SO_4{\cdot}10H_2O$ $CaSO_4{\cdot}2H_2O$
M15	$Ca(NO_3)_2{\cdot}4H_2O$ $MgSO_4{\cdot}7H_2O$	$CaSO_4{\cdot}2H_2O$	$NaNO_3$; $Ca(NO_3)_2{\cdot}4H_2O$ $MgSO_4{\cdot}7H_2O$ $CaSO_4{\cdot}2H_2O$	$MgSO_4{\cdot}7H_2O$ $CaSO_4{\cdot}2H_2O$	$Ca(NO_3)_2{\cdot}4H_2O$ $MgSO_4{\cdot}7H_2O$	$CaSO_4{\cdot}2H_2O$
M16	$CaSO_4{\cdot}2H_2O$	$MgSO_4{\cdot}7H_2O$	Na_2SO_4	Low crystallinity sulfates ↓↓	–	–
M17	$NaNO_3$; $Ca(NO_3)_2{\cdot}4H_2O$ $MgSO_4{\cdot}7H_2O$ $CaSO_4{\cdot}2H_2O$	$Na_2SO_4{\cdot}10H_2O$ $NaNO_3$; $Ca(NO_3)_2{\cdot}4H_2O$ $MgSO_4{\cdot}7H_2O$ $CaSO_4{\cdot}2H_2O$	–	$Na_2SO_4{\cdot}10H_2O$	–	–

$MgSO_4{\cdot}7H_2O$: epsomite; $CaSO_4{\cdot}2H_2O$: gypsum; $NaNO_3$: nitratine; $Na_2SO_4{\cdot}10H_2O$: mirabilite; Na_2SO_4: thenardite; $Ca(NO_3)_2{\cdot}4H_2O$: nitrocalcite.

As a rule, the mortars were readily applied and removed when the layer was around 2 cm thick. They bonded well in all cases, with no detachments after 10 days. Removal was not fully effective, however, for small amounts remained attached to the wall.

Since the mineralogical study of the salts removed showed that they consisted of sulfates and nitrates, the content of these two salts, together with the chloride ion, which is not detectable with Raman spectroscopy, was analysed with IC techniques.

Figs. 6–8 show the soluble nitrates, chlorides and sulfates present in the stones at the three depths before and after the first and the third applications of the desalinating mortars and 3 yr after treatment.

The nitrates were eliminated very effectively even after the first application of mortars M15 and M14, whilst nitrate extraction was small in mortars M16 and M17, as would be expected given the lower initial content of these salts. These data were consistent with the Raman findings on the salts present in the mortars. Table 10 gives the variation in the anions analysed at different depths after mortar application, expressed as the percentage of the salt content prior to each application.

Mortar efficacy in removing sulfates also varied. Mortars M16 and M14 (applied in areas with a smaller initial sulfate content) lowered the concentration in the stone at all three investigated depths from the very first application and improved the results after the second (Table 10). M15 and M17 (applied to areas with a higher initial sulfate content) mobilised these anions, drawing them from the deeper areas of the stone to the surface and extracting them, as the Raman studies of the inner and outer sides of the mortars showed. As they were unable to remove all the sulfates mobilised from the stone after three applications, however, the stone had higher sulfate concentrations at 0.5 cm and 1.5 cm from the surface than before the trial. These findings confirmed the need to study the origin of soluble salts and eradicate their source prior to removal.

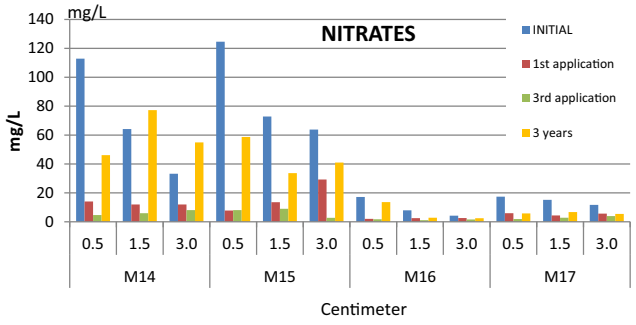

Fig. 6. Nitrate concentration at different depths in ashlars before and after the first and the third of desalinating mortars and 3 years after the last desalination.

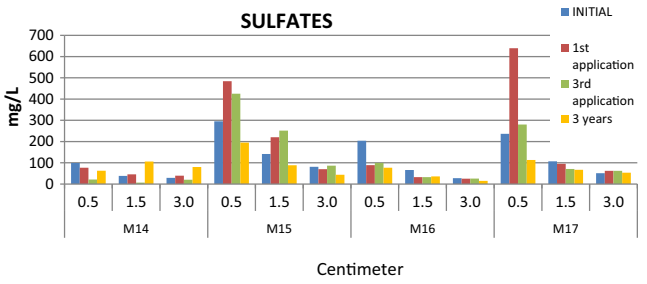

Fig. 7. Sulfate concentration at different depths in ashlars before and after the application of desalinating mortars and 3 years after the last desalination.

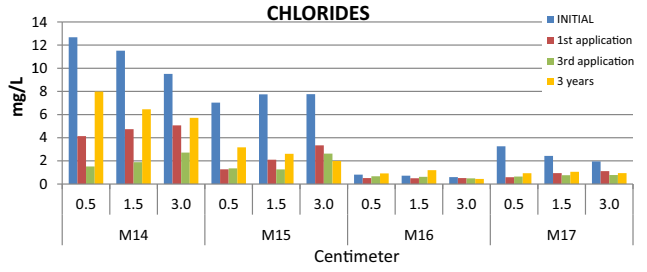

Fig. 8. Chloride concentration at different depths in ashlars before and after the application of desalinating mortars and 3 yr after the last desalination.

Chloride concentration declined after the first application. The effect was minor in the second except for in mortar M14, where the content at 0.5 cm declined by 63% and at 1.5 cm by 60% (Table 10). Mortars M15 and M17 lowered the percentage of salts most effectively after the first application, whilst mortar M16 was ineffective.

While the appearance of the selected ashlars it was similar, that is, they were covered with efflorescence, and although they were mechanically eliminated in the same way, according to the results, the salts are not distributed homogeneously in the different ashlars, varying their initial concentration (in the first 0.5 cm deep

Table 10
Percentage variation in anion content at different depths after the first and third application of mortars and 3 yr later.

(wt%)	M15			M16			M17			M14		
Depth (cm)	0.5	1.5	3.0	0.5	1.5	3.0	0.5	1.5	3.0	0.5	1.5	3.0
Nitrates												
1st application	−88	−81	−64	−94	−81	−54	−88	−68	−39	−66	−71	−51
3nd application	−67	−51	−33	4	−33	−91	−16	−55	−38	−69	−36	−30
After 3 yr	−59	20	65	−53	−54	−36	−20	−64	−42	−67	−55	−54
Sulfates												
1st application	−23	19	34	64	55	−14	−56	−50	−9	170	−11	21
3nd application	−72	−85	−48	−12	14	23	12	−1	2	−56	−26	0
Third year	−37	176	173	−34	−37	−46	−62	−45	−46	−52	−37	5
Chlorides												
1st application	−67	−59	−47	−82	−73	−57	−37	−31	−13	−82	−61	−43
3nd application	−63	−60	−46	6	−40	−21	30	24	−6	10	−19	−30
After 3 yr	−37	−44	−40	−55	−66	−74	13	67	−26	−71	−56	−52

Table 11
Total anion concentration in ashlars: before and 3 yr after the last desalination.

	M14 (initial)	M14 (3 year)	M15 (initial)	M15 (3 year)	M16 (initial)	M16 (3 year)	M17 (initial)	M17 (3 year)
Nitrates (mg/L)	210	178	261	133	29	19	44	18
Sulfates (mg/L)	167	249	518	327	297	128	395	234
Chlorides (mg/L)	33.7	20.2	22.5	7.8	2.1	2.6	7.6	2.9
Total (mg/L)	410.7	447.2	801.5	467.8	328.1	149.6	446.6	254.9

of the different selected ashlar) between 10 and 100 ppm in the case of nitrates, between 80 and 300 ppm of sulfates and chlorides between 1 and 13 ppm.

Consequently, the effectiveness of mortars depends not only on their porosity and distribution of pore size but also, and to a large extent, on the amount of salts in the stone. If you look at the evolution of the concentration of sulfates, the mortars M14 and M15, with similar porosity and pore size distribution, behave very differently. The M14 mortar effectively reduces the concentration of sulfates at all the three depths, a fact that is not observed in the case of M15. Therefore, the M15 mortar extracted and mobilised more salts in absolute value, but having a very high initial concentration, part of the mobilised sulfates were concentrated in more superficial areas. Hence, its lower efficiency is only apparent.

The concentration of the most mobile anions, i.e., chlorides and nitrates, rose again three years after desalination treatment at the three investigated depths, if compared to the values found after the third application of the desalinating mortars, an indication that the source of these salts remained active. Despite such a rise, the salt content in all areas was lower than before treatment except where mortar M14 was applied. In all other cases, the content after 3 yr was around 50% of the initial value (Table 11).

4. Conclusions

Four absorbent mortars were designed in this study and used as sacrificial desalinating media. The mortars designed comprised lime, sepiolite, nanosilica (72/3/25 by weight) and three admixtures (H_2O_2 and two commercial aerators). The liquid/solid ratio was 0.9, porosity 40% and the mean pore size 0.8–0.7 μm. These mortars were applied three times to ashlars on a church wall affected by salts and their desalinating efficacy by number of applications was studied at depths of 0.5 cm, 1.5 cm and 3.0 cm from the surface.

When laid to a thickness of 2 cm, the mortars bonded well to the substrate for 10 days but loosely enough to be removed by hand, leaving scantly any trace on the wall.

All the mortars mobilised and absorbed soluble salts in the ashlars, eliminating ions with a small ionic volume and high mobility, especially chlorides and nitrates, more effectively. Sulfates, with a larger ionic volume, were also mobilised to the ashlar surface from the deepest depth studied, thereby raising the surface concentration of these salts. However, the anions mobilised were not fully eliminated after the third cycle of applications of the desalinating mortars.

As a rule, the mortars were more effective when the salt concentration in the wall was high and superficial. Inasmuch as nitrates and chlorides were most effectively eliminated after the first application, the suitability or otherwise of a second would need to be explored. A third application was necessary to eliminate sulfates, for the sulfate content from inside the wall rose at first.

Three years after the last application, the salt concentration was just half of the value observed in the areas where all but one of the mortars were applied. The exception was the area treated with admixture-free mortar M14, where the before and after salt content were similar.

Conflict of interest

There is no conflict of interest.

Acknowledgements

This study was funded by the Regional Government of Madrid's 'Geomateriales 2' programme (S2013/MIT2914) under the CLIMORTEC project (BIA2014-53911-R).

The assistance provided by the Archbishopric of Alcalá de Henares, Madrid, and all the people associated with the Talamanca del Jarama church is gratefully acknowledged.

The authors want to thanks Sika for the supply of aerators.

References

[1] A. Arnold, K. Zehnder, Monitoring wall paintings affected by soluble salts, in: S. Cather (Ed.), The Conservation of Wall Paintings, Los Angeles, The Getty Conservation Institute, 1991.

[2] A.S. Goudie, H.A. Viles, Salt Weathering Hazards, Wiley, Chichester, 1997.
[3] L. Falchi, E. Zendri, E. Capovilla, P. Romagnoni, M. De Bei, The behaviour of water-repellent mortars with regards to salt crystallization: from mortar specimens to masonry/render systems, Mater Struct. 50 (2017) 66, https://doi.org/10.1617/s11527-016-0891-8.
[4] M.J. Varas-Muriel, R. Fort, M.I. Martinez-Garrido, A. Zornoza-Indart, P. Lopez-Arce, Fluctuations in the indoor environment in Spanish rural churches and their effects on heritage conservation: hygro-thermal and CO2 conditions monitoring, Build. Environ. 82 (2014) 97–109, https://doi.org/10.1155/2016/1280894.
[5] A. Sawdy, B. Lubelli, V. Voronina, F. Funke, L. Pel, Optimising the extraction of soluble salts from porous materials by poultices, Stud. Conserv. 55 (2010) 26–40, https://doi.org/10.1179/sic.2010.55.1.26-.
[6] B. Lubelli, R.P.J. van Hess, Desalination of masonry structures: fine tuning of pore size distribution of poultices to substrate properties, J. Cult. Heritage 11 (1) (2010) 10–18, https://doi.org/10.1016/j.culher.2009.03.005.
[7] V. Voronina, L. Pel, K. Kopinga, Effect of osmotic pressure on salt extraction by a poultice, Constr. Build. Mater. 53 (2014) 432–438, https://doi.org/10.1016/j.conbuildmat.2013.10.071.
[8] S. Kroener, B.M. Alcaide, X. Mas-Barbera, Influence of substrate pore size distribution, poultice type, and application technique on the desalination of medium-porous stones, Stud. Conserv. 61 (5) (2016) 286–296, https://doi.org/10.1080/00393630.2015.1131942.
[9] C. Selwitz, E. Doehne, The evaluation of crystallization modifiers for controlling salt damage to limestone, J. Cult. Heritage 3 (3) (2002) 205–216, https://doi.org/10.1016/S1296-2074(02)01182-2.
[10] P. López-Arce, M.J. Varas-Muriel, B. Fernández-Revuelta, M. Álvarez de Buergo, R. Fort, C. Pérez-Soba, Artificial weathering of Spanish granites subjected to salt crystallization tests: surface roughness quantification, Catena 83 (2–3) (2010) 170–185, https://doi.org/10.1016/j.catena.2010.08.009.
[11] M.F. La Russa, S.A. Ruffolo, C.M. Belfiore, P. Aloise, L. Randazzo, N. Rovella, A. Pezzino, G. Montana, Study of the effects of salt crystallization on degradation of limestone rocks, Periodico di Mineralogia 82 (1) (2013) 113–127, https://doi.org/10.2451/2013PM0007.
[12] E. Franzoni, Rising damp removal from historical masonries: a still open challenge, Constr. Build. Mater. 54 (2014) 123–136, https://doi.org/10.1016/j.conbuildmat.2013.12.054.
[13] C. Alves, J. Sanjurjo-Sanchez, Conservation of stony materials in the built environment, Environ. Chem. Lett. 13 (4) (2015) 413–430, https://doi.org/10.1007/s10311-015-0526-2.
[14] B. Lubelli, R.P.J. van Hees, Effectiveness of crystallization inhibitors in preventing salt damage in building materials, J. Cult. Heritage 8 (3) (2007) 223–234, https://doi.org/10.1016/j.culher.2007.06.001.
[15] I. Egartner, O. Sass, Using paper pulp poultices in the field and laboratory to analyse salt distribution in building limestones, Heritage Sci. (4) (2016) 41, https://doi.org/10.1186/s40494-016-0110-5.
[16] J. Delgado, A.S. Guimaraes, V.P. de Freitas, I. Antepara, V. Kolí, R. Herný, Salt damage and rising damp treatment in building structures, Adv. Mater Sci. Eng. (2016) 13, https://doi.org/10.1155/2016/1280894.
[17] J. Feijoo, O. Matyscak, L.M. Ottosen, Novoa XR RivasT, Electrokinetic desalination of protruded areas of stone avoiding the direct contact with electrodes, Mater Struct. 50 (2017) 82, https://doi.org/10.1617/s11527-016-0946-x.
[18] V. Vergés-Belmin, H. Siedel, Desalination of masonries and monumental sculptures by poulticing: a review, Restor. Build. Monuments: Int. J. 11 (6) (2005) 391–408, https://doi.org/10.1515/rbm-2005-6000.
[19] L. Pel, A. Sawdy, V. Voronina, Physical principles and efficiency of salt extraction by poulticing, J. Cult Heritage 11 (1) (2010) 59–67, https://doi.org/10.1016/j.culher.2009.03.007.
[20] P. López-Arce, R. Fort, M. Gómez-Heras, E. Perez-Monserrat, M.J. Varas, Preservation strategies for avoidance of salt crystallisation in El Paular Monastery cloister, Madrid, Spain, Environ. Earth Sci. 63 (2011) 1487–1509, https://doi.org/10.1007/s12665-010-0733-x.
[21] V. Fassina, M. Favaro, A. Naccari, M. Pigo, Evaluation of compatibility and durability of a hydraulic lime-based plaster applied on brick wall masonry of historical buildings affected by rising damp phenomena, J. Cult. Heritage 3 (1) (2002) 45–51, https://doi.org/10.1016/S1296-2074(02)01158-5.
[22] J. Setina, L. Krage, J. Svare, S. Kirilova, Simulation of desalination processes using lime based mortars, Chem. Technol. 1 (2009) 30–35. http://www.chemija.ctf.ktu.lt/zurnalas/pdf/50-06-Setina.pdf.
[23] A. Bourges, V. Verges-Belmin, Application of fresh mortar tests to poultices used for the desalination of historical. masonry, Mater. Struct. 44 (7) (2011) 1233–1240, https://doi.org/10.1617/s11527-010-9695-4.
[24] S. Martínez-Ramírez, F. Puertas, M.T. Blanco-Varela, Carbonation process and properties of a new lime mortar with added sepiolite, Cem. Concr. Res. 25 (1) (1995) 39–50, https://doi.org/10.1016/0008-8846(94)00110-K.
[25] S. Martínez-Ramírez, F. Puertas, M.T. Blanco-Varela, G.E. Thompson, Effect of dry deposition of pollutants on the degradation of lime mortars with sepiolite, Cem. Concr. Compos. 28 (1) (1998) 125–133, https://doi.org/10.1016/S0008-8846(97)00255-X.
[26] I.F. Sáez del Bosque, M. Martín-Pastor, S. Martínez- Ramírez, M.T. Blanco-Varela, Effect of temperature on C_3S and C_3S+ nanosilica hydration and C-S-H gel structure, J. Am. Ceram. Soc. 96 (2013) 957–965, https://doi.org/10.1111/jace.12093.
[27] I. Navarro-Blasco, J.I. Álvarez, Obtaining repair lime mortars by mixing aerial lime and nanosilica, in: 3rd Historic Mortars Conference, 11-14 September, Glasgow, Scotland (UK), 2013.
[28] A.M. Neville, Properties of Concrete, Addison Wesley Longman Limited, Essex, 1995.
[29] B. Keertana, S.S. Mani, M. Thenmozhi, Utilization of ecosand and fly ash in aerated concrete for a richest mix design, Int. J. Eng Sci Technol. 3 (1) (2011) 299–304.
[30] R. Fort, M. Álvarez de Buergo, E. Pérez-Monserrat, M. Gómez-Heras, M.J. Varas, D.M. Freire, Evolution in the use of natural building stone in Madrid, Spain, Q. J. Eng. Geol. Hydrogr. 46 (4) (2013) 421–429, https://doi.org/10.1144/qjegh2012-041.
[31] R. Fort, B. Fernández-Revuelta, M.J. Varas, M. Álvarez de Buergo, M. Taborda, Influence of anisotropy on the durability of Madrid-region Cretaceous dolostone exposed to salt crystallization processes, Mater. Constr. 58 (2008) 289–290.
[32] M.I. Martínez-Garrido, S. Aparicio, R. Fort, M.A.G. Izquierdo, J.J. Ayala, Effect of solar radiation and humidity on the inner core of walls in historic buildings, Constr. Build. Mater. 51 (2014) 384–395.
[33] EN 16302:2012. Conservation of Cultural Heritage. Test methods. Measurement of water absorption by pipe method.
[34] UNE-EN 1925:1999 Determination of water absorption coefficient by capillarity.
[35] RILEM (1980). Recommended tests to measure the deterioration of stone and to assess the effectiveness of treatment methods. Comission 25-PEM: Protection et Érosion des Monuments, 175–253.
[36] M.J. Varas-Muriel, E.M. Perez-Monserrat, C. Vazquez-Calvo, R. For, Effect of conservation treatments on heritage stone. Characterisation of decay processes in a case study, Constr. Build. Mater. 95 (2015) 611–622, https://doi.org/10.1016/j.conbuildmat.2015.07.087.
[37] A. Wang, J.J. Freeman, B.L. Jolliff, I.M. Chou, Sulfates on mars: a systematic Raman spectroscopic study of hydration states of magnesium sulfates, Geochim. Cosmochim. 70 (2006) 6118–6135, https://doi.org/10.1016/j.gca.2006.05.022.